Uncoupling Cell Fate Determination from Patterned Cell Division in the *Drosophila* Eye

Joriene C. de Nooij and Iswar K. Hariharan*

Cell proliferation and cell fate specification are under strict spatiotemporal control in the developing *Drosophila* eye. Cells excluded from five-cell preclusters synchronously enter a single additional cell cycle, the second mitotic wave, after which the remaining cells are sequentially recruited. When the second mitotic wave was blocked with the human cyclin-dependent kinase inhibitor $p21^{CIP1/WAF1}$, each cell type was still specified. Hence, cell fate determination is regulated independently of the division pattern of precursor cells. However, the second mitotic wave is needed to generate appropriate numbers of each cell type. Moreover, p21 can arrest precursor cell proliferation and allow appropriate fate choice in vivo.

During the development of many organisms, precursor cells undergo characteristic patterns of cell division before commitment to specific fates. Such invariant divisions may result from the dependence of cell fate on cell lineage; a precise pattern of divisions may be necessary to achieve the required distribution of cytoplasmic determinants (*1*). However, in some cases, cell division is tightly controlled even though cells adopt fates independently of their lineage history (*2*, *3*). Here, we investigated the requirement for patterned cell divisions in one such system, the developing eye of *Drosophila*.

In the eye imaginal disc, asynchronous cell divisions precede the morphogenetic furrow, an anteriorly moving dorsoventral indentation that marks the onset of pattern formation. Posterior to the furrow, regularly spaced groups of five cells stop dividing and are specified as photoreceptor cells R8, R2, R5, R3, and R4 (*3*–*5*). Every cell that is excluded from the precluster undergoes a single and highly synchronous S phase posterior to the furrow. Cells derived from this second mitotic wave represent the precursor pool from which the photoreceptor cells R1, R6, and R7, the cone cells, the pigment cells, and finally the precursors of the mechanosensory bristles are sequentially recruited. The remaining unspecified cells undergo apoptosis (*6*).

To ascertain whether cell division during the second mitotic wave functions in programming cell fates, we generated lines of *Drosophila* in which this last round of cell division was specifically blocked. The human cyclin-dependent kinase inhibitor $p21^{CIP1/WAF1}$ (*7*, *8*) arrests the proliferation of cycling mammalian cells in culture. We used the *pGMR* promoter (*9*) to target expression of the *p21* gene to cells posterior to the morphogenetic furrow in the eye imaginal disc (Fig. 1A). Nine independent transgenic lines were generated, each of which displayed similar phenotypic abnormalities (*10*). Expression of the transgene in cells posterior to the furrow in the eye imaginal disc was confirmed with antibody to p21 (anti-p21) (*11*).

To determine the effect of the *p21* transgene on the pattern of cell division, we dissected eye antennal discs from third instar larvae and incubated them in 5-bromo-2′-deoxyuridine (BrdU) to label nuclei in the S phase of the cell cycle (Fig. 1, B and C). In wild-type discs, BrdU incorporation was seen anterior to the morphogenetic furrow, in a clear stripe just posterior to the furrow (the second mitotic wave) and at a more basal level, in the nuclei of cells associated with the optic nerve. In discs derived from the transgenic line $GMRp21^{B}$, the second mitotic wave was completely abolished. However, labeled nuclei were still observed both anterior to the morphogenetic furrow and in cells associated with the optic nerve, regions where the transgene was not expressed. Thus, expression of p21 is able to prevent the G_1-arrested cells posterior to the furrow from entering S phase.

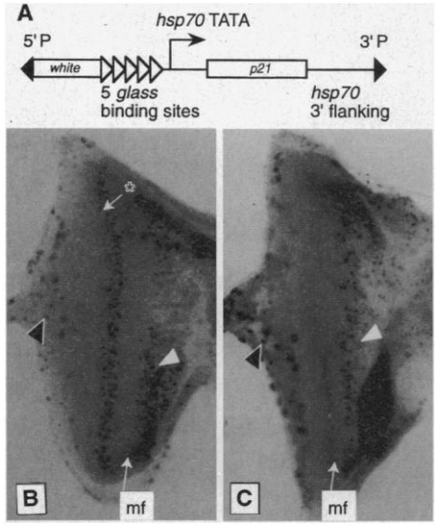

Fig. 1. Expression of p21 posterior to the morphogenetic furrow abolishes the second mitotic wave. (**A**) Structure of the *GMRp21* construct used to generate transgenic *Drosophila* (not drawn to scale). The *glass* binding sites direct transcription of *p21* to all cells posterior to the morphogenetic furrow in the eye imaginal disc (*9*). Eye imaginal discs from a wild-type fly (**B**) and from a fly bearing two copies of the *GMRp21* gene ($GMRp21^{B}$/+) (**C**) were incubated with BrdU (*16*) (anterior is to the right; mf, morphogenetic furrow). In wild-type discs, nuclei are labeled anterior to the morphogenetic furrow (white arrowhead), in the second mitotic wave (asterisk), and in cells associated with the optic nerve (black arrowhead). Discs from $GMRp21^{B}$ flies have no detectable second mitotic wave. Magnification: ×200.

We compared adult eyes from wild-type and mutant flies by scanning electron microscopy (SEM) and by analysis of retinal sections (Fig. 2) to assess the consequences of blocking the second mitotic wave. In wild-type flies, the adult eye is composed of a regular array of eight photoreceptor cells, four cone cells, pigment cells that separate adjacent ommatidia, and interommatidial mechanosensory bristles. Photoreceptors R1, R6, and R7, the cone cells, the pigment cells, and the bristle precursors are normally derived from cells generated by the second mitotic wave (*3*, *5*). SEM micrographs of mutant eyes (Fig. 2, B and D) indicated irregularity of the ommatidial architecture as well as a large reduction in the number of interommatidial bristles (typically 15% of the wild-type number). Retinal sections of $GMRp21^{B}$ flies indicated that almost all (>98%) of the ommatidia contained the full complement of photoreceptor cells (Fig. 2, E and F). In contrast, many pigment cells were missing; only 13% of the ommatidia were fully surrounded by pigment cells. Hence, despite complete abrogation of the second mitotic wave, all the specialized cell types of the normal retina were determined correctly. However, although cell types that are normally determined soon after the second wave (photoreceptors R1, R6, and R7) were fully represented, those determined later (pigment cells, bristle cells) were severely underrepresented.

To examine the specification of each of the specialized cell types during development, we examined larval and pupal eye imaginal discs with the use of several cell type–specific markers. Developing photoreceptor cell nuclei were identified by staining larval and pupal imaginal discs with an antibody to the elav antigen, which is expressed in the nuclei of neuronal cells (*12*). Each cluster contains the normal complement of staining nuclei, although in the $GMRp21^{B}$ pupal discs not all of the nuclei are aligned in the same focal plane (Fig. 3,

J. C. de Nooij, Massachusetts General Hospital Cancer Center, Building 149, 13th Street, Charlestown, MA 02129, USA.
I. K. Hariharan, Massachusetts General Hospital Cancer Center and Harvard Medical School, Building 149, 13th Street, Charlestown, MA 02129, USA.
*To whom correspondence should be addressed.

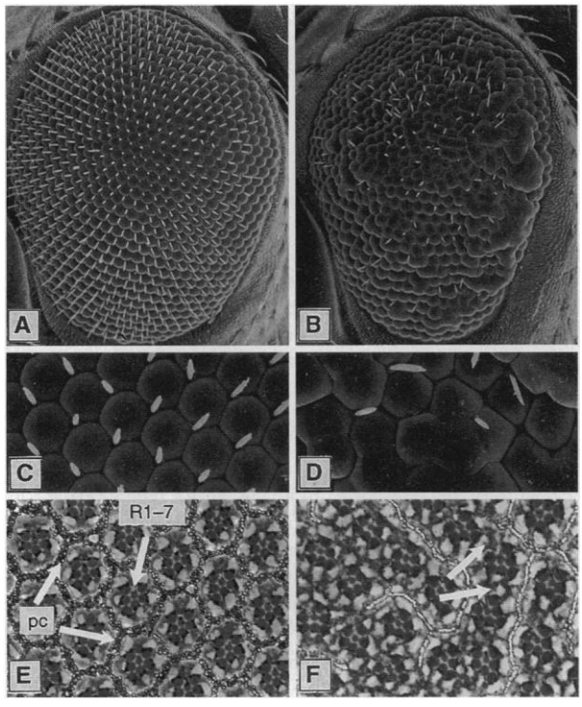

Fig. 2. Expression of p21 disrupts eye structure. (**A** through **D**) SEM micrographs (*17*) of eyes from wild-type flies (A and C) and transgenic flies (B and D). (**E** and **F**) Adult sections from wild-type flies (E) and transgenic flies (F). In (E), R1–7 indicates the rhabdomeres of the photoreceptor cells R1 through R7; pc indicates a pigment cell. Arrows in (F) indicate the locations of missing pigment cells. Magnifications: ×125 (A and B), ×550 (C and D), ×625 (E and F).

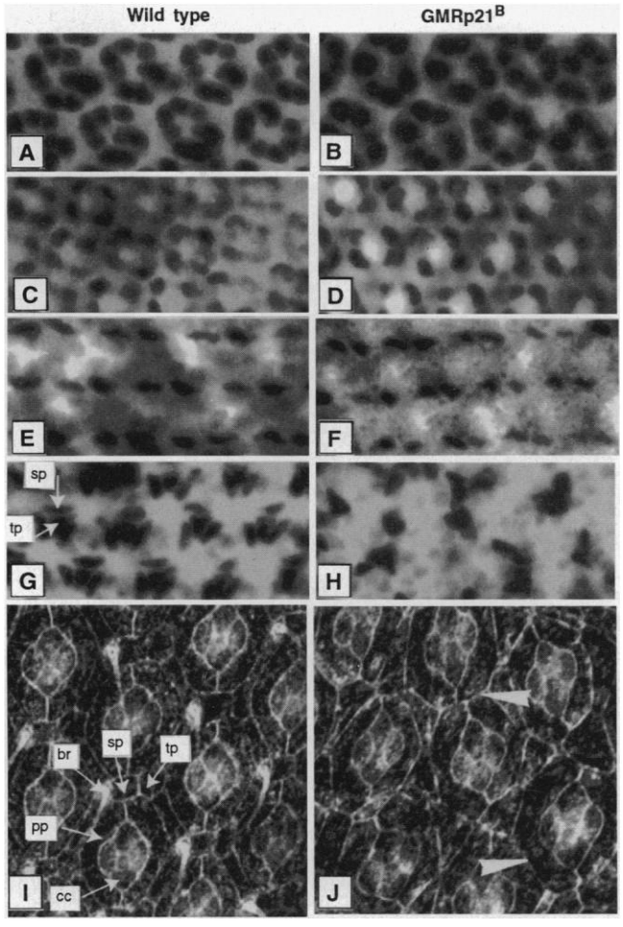

Fig. 3. Expression of p21 disrupts eye development. Preparations were made from wild-type pupal retinas (**A**, **C**, **E**, **G**, and **I**) and from *GMRp21^{B}*/+ pupal retinas (**B**, **D**, **F**, **H**, and **J**). Eye discs from 40-hour-old pupae (aged at 25°C) were dissected and stained with anti-elav to identify nuclei of photoreceptor cells (A and B). The enhancer trap line P191, which expresses β-galactosidase in the nuclei of cone cells and all pigment cells, was crossed to wild-type and GMRp21^{B} transgenic flies, and tissues from these crosses were stained with anti–β-galactosidase (*9*). Nuclei were identified by their shape, arrangement, and position in the retina. The cone cell nuclei (C and D), the primary pigment cell nuclei (E and F), and the nuclei of the secondary and tertiary pigment cells (G and H) are shown. In (I) and (J), pupal retinas were stained with rhodamine-conjugated phalloidin and visualized by confocal microscopy (*17*). Symbols in (G) and (I): sp, secondary pigment cell; tp, tertiary pigment cell; cc, cone cell; pp, primary pigment cell; and br, interommatidial bristle. In (J), the arrowheads indicate direct contact between primary pigment cells from adjacent ommatidia. Magnifications: ×650 (A through H), ×1000 (I and J).

A and B). The development of cone cells and pigment cells was examined with the use of an enhancer trap line, P191, which expresses β-galactosidase in the nuclei of these cells (Fig. 3, C through H). Although each ommatidium from the GMRp21^{B} discs contained the normal complement of cone cells (Fig. 3, C and D) and primary pigment cells (Fig. 3, E and F), many secondary and tertiary pigment cells were missing (Fig. 3, G and H). This absence was especially evident in pupal retinas stained with phalloidin, which stains cortical actin and demarcates cell outlines (Fig. 3, I and J). Almost all ommatidia from the GMRp21^{B} eyes contained the normal complement of four cone cells and two primary pigment cells. In wild-type retinas, the primary pigment cells of each ommatidial cluster are surrounded by a ring of cells consisting of the secondary and tertiary pigment cells and the interommatidial bristles. In the GMRp21^{B} retinas, far fewer cells were found between adjacent ommatidia. Indeed, in some instances, the primary pigment cells of adjacent ommatidia were directly apposed (Fig. 3J). The GMRp21^{B} retinas also lacked most of the interommatidial bristles. Hence, in the absence of the second mitotic wave, the specification of most cell types occurred normally until the final stages, when many pigment cells and bristle cells were missing, presumably because of a deficit of precursor cells. Moreover, although the remaining unspecified cells undergo apoptosis in wild-type retinas, apoptosis was greatly reduced in GMRp21^{B} retinas (*11*), consistent with the notion that all the available precursor cells were used up.

We have shown that even though precursor cells undergo divisions in a stereotypic manner during retinal development, cell fate specification is not dependent on the pattern of precursor cell division. Hence, the two processes must be organized independently. Although the arrested cells are unable to progress through the second mitotic wave, they can generate each of the specialized cell types found in the adult retina, and these cells are incorporated appropriately into developing ommatidia. However, without the second mitotic wave, the retina lacks the full complement of precursor cells and is therefore unable to complete its development. Thus, the final division is not necessary for the programming of individual cell fates, but it is necessary for the generation of sufficient precursor cells from which all the cells required for each ommatidium can be recruited.

Our experiments also address the properties of the cyclin-dependent kinase inhibitor p21 in vivo. Cells are arrested in the G_1 phase of the cell cycle in the morphogenetic furrow (*13*). Expression of p21 in these cells prevented them from reentering the

cell cycle and abolished the second mitotic wave. The arrested cells were not forced to differentiate along any single pathway. Rather, they could respond to physiological differentiation signals and could adopt a variety of cell fates as they were sequentially recruited to the developing ommatidia. Hence, the expression of p21 does not drive differentiation, but rather maintains precursor cells in a state that permits differentiation. In cultured mammalian cells and in mouse embryos, p21 is expressed in cells as they cease to proliferate and begin to differentiate (*14*). Thus, p21 is likely to function in the developmental switch from proliferation to differentiation.

Although p21 homologs have not yet been found in nonmammalian species, homologs of the cyclins and cyclin-dependent kinases have been found in *Drosophila* (*15*). The ability of human p21 to inhibit *Drosophila* cells from entering S phase suggests that the mechanisms of inhibition of the cyclin-dependent kinases are general and conserved across species. Finally, the ability of human p21 to function in diverse species indicates its utility as an experimental tool for arresting the division of specific populations of cells in vivo.

REFERENCES AND NOTES

1. S. Strome and W. B. Wood, *Cell* **35**, 15 (1983); M. S. Rhyu, L. Y. Jan, Y. N. Jan, *ibid.* **76**, 477 (1994); B. Bowerman, B. W. Draper, C. C. Mello, J. R. Preiss, *ibid.* **74**, 443 (1993).
2. V. E. Foe, *Development* **107**, 1 (1989).
3. D. F. Ready, T. E. Hanson, S. Benzer, *Dev. Biol.* **53**, 217 (1976).
4. J. A. Campos-Ortega, in *Current Topics in Developmental Biology*, A. A. Moscona and A. Monroy, Eds. (Academic Press, New York, 1980), vol. 15, pp. 347–371.
5. T. Wolff and D. F. Ready, *Development* **113**, 841 (1991).
6. ———, *ibid.*, p. 825.
7. A. Noda, Y. Ning, S. F. Venable, O. M. Pereira-Smith, J. R. Smith, *Exp. Cell. Res.* **211**, 90 (1994); J. W. Harper, G. R. Adami, N. Wei, K. Keyomarsi, S. J. Elledge, *Cell* **75**, 805 (1993); Y. Xiong *et al.*, *Nature* **366**, 701 (1993).
8. W. S. El-Deiry *et al.*, *Cell* **75**, 817 (1993).
9. B. A. Hay, T. Wolff, G. M. Rubin, *Development* **120**, 2121 (1994); M. C. Ellis, E. M. O'Neill, G. M. Rubin, *ibid.* **119**, 855 (1993).
10. The *p21* complementary DNA (cDNA) contains sequences from 1 to 2005 base pairs (*8*) cloned into the Stu I site of *pGMR*. Nine independent transgenic lines were generated. Flies with two or more copies of the *GMRp21* transgene displayed rough eyes and lacked the second mitotic wave. Most experiments were conducted with GMRp21^{B} flies, which were heterozygous for a chromosome bearing two independent integrations of the transgene.
11. J. C. de Nooij and I. K. Hariharan, unpublished data.
12. S. Robinow and K. White, *Dev. Biol.* **126**, 294 (1988).
13. B. J. Thomas, D. A. Gunning, J. Cho, S. L. Zipursky, *Cell* **77**, 1003 (1994).
14. O. Halevy *et al.*, *Science* **267**, 1018 (1995); H. Jiang *et al.*, *Oncogene* **9**, 3397 (1994); S. B. Parker *et al.*, *Science* **267**, 1024 (1995).
15. C. F. Lehner and P. H. O'Farrell, *EMBO J.* **9**, 3573 (1990); J. Jimenez, L. Alphey, P. Nurse, D. M. Glover, *ibid.*, p. 3565; C. F. Lehner and P. H. O'Farrell, *Cell* **56**, 957 (1989); *ibid.* **61**, 535 (1990); W. G. F. Whitfield, C. Gonzalez, G. Maldonado-Codina, D. M. Glover, *EMBO J.* **9**, 2563 (1990). H. E. Richardson, L. V. O'Keefe, S. I. Reed, R. Saint, *Development* **119**, 673 (1993).
16. To visualize nuclei in S phase, we dissected third-instar larval discs in Schneider's medium; the discs were incubated in BrdU (0.3 mg/ml) for 1 hour at 20°C, washed, fixed in 4% paraformaldehyde in PEM [0.1 M Pipes (pH 7.0), 1 mM EGTA, and 2 mM $MgSO_4$] [B. E. Kimmel, U. Heberlein, G. M. Rubin, *Genes Dev.* **4**, 712 (1990)] for 30 min at 20°C, washed in phosphate-buffered saline with 0.3% Triton X-100 (PBT) and incubated in 2 M HCl in PBT for 30 min at 20°C, washed in PBT again, incubated overnight in anti-BrdU (Becton-Dickinson, 1:100), and then visualized by histochemical staining [A. Tomlinson and D. F. Ready, *Dev. Biol.* **120**, 336 (1987)].
17. I. K. Hariharan *et al.*, *EMBO J.* **14**, 292 (1995).

18. We thank J. Koh for the *p21* cDNA, B. Dynlacht for anti-p21, the G. M. Rubin laboratory for anti-elav, R. Cagan for the enhancer trap line P191, E. Seling for help with the SEM, R. Simmons for technical assistance, and B. Dynlacht, B. Hay, U. Heberlein, R. Singh, J. Treisman, J. Vize, and T. Wolff for comments. Supported by grants from the American Cancer Society (DB-75) and the G. Harold and Leila Y. Mathers Charitable Foundation.

27 July 1995; accepted 17 October 1995

Lymphoproliferative Disorders with Early Lethality in Mice Deficient in *Ctla-4*

Paul Waterhouse, Josef M. Penninger, Emma Timms, Andrew Wakeham, Arda Shahinian, Kelvin P. Lee, Craig B. Thompson, Henrik Griesser, Tak W. Mak*

The role of the cell-surface molecule CTLA-4 in the regulation of T cell activation has been controversial. Here, lymph nodes and spleens of CTLA-4–deficient mice accumulated T cell blasts with up-regulated activation markers. These blast cells also infiltrated liver, heart, lung, and pancreas tissue, and amounts of serum immunoglobulin were elevated. The mice invariably became moribund by 3 to 4 weeks of age. Although CTLA-4–deficient T cells proliferated spontaneously and strongly when stimulated through the T cell receptor, they were sensitive to cell death induced by cross-linking of the Fas receptor and by gamma irradiation. Thus, CTLA-4 acts as a negative regulator of T cell activation and is vital for the control of lymphocyte homeostasis.

The CTLA-4 receptor has been postulated to play a regulatory role in T cell activation largely on the basis of its similarity to the costimulatory receptor CD28 (*1*). Mouse *Ctla-4* complementary DNA (*2*) is 76% identical in sequence to CD28, and both are located in close proximity on chromosome 1 (*3*). CD28 is found on essentially all resting T cells and can augment the response of antigen-activated T cells (*1*). In contrast, CTLA-4 is not expressed on resting T cells but is detectable on activated T cells after antigen activation (*4*). Although a role for CD28 in augmenting T cell–dependent responses is well established, antibody blocking or cross-linking of CTLA-4 has yielded contradictory results (*4*, *5*). Interpretation of these studies is complicated by the fact that CD28 and CTLA-4 bind to the same ligands B7-1 (CD80) and B7-2 (CD86) (*6*). The shared ligands and the complex expression patterns of both receptors and ligands make it difficult to address definitively the role of CTLA-4. Here, we show that gene-targeted mice lacking CTLA-4 progressively accumulate T cell blasts, which indicates that CTLA-4 is a negative regulator.

A gene-targeting construct (Fig. 1A) was generated (*7*). The construct was electroporated into E14 embryonic stem (ES) cells, the targeted ES clones (Fig. 1B) injected into C57BL/6 blastocysts, and the resulting chimeras bred to C57BL/6 females. Tail DNA of agouti pups showed transmission of the targeted allele (Fig. 1B). T cells were double-stained for αβ T cell receptor (TCRαβ) and either CTLA-4 or one of the activation markers CD25, CD44, or CD69. Activated T cells from *Ctla-4*$^{-/-}$ mice do not express *Ctla-4* but had high levels of expression of these activation markers (Fig. 1C).

Mice heterozygous for the *Ctla-4* mutation appeared normal. Homozygous mice were born at the expected Mendelian frequency and appeared healthy at birth. However, by 2 weeks of age they became sick and became moribund at 3 to 4 weeks of age. The spleen and all lymph nodes were 5 to 10 times the normal size, reflected by an increase in the number of lymphocytes (Table 1). Histology revealed extensive accumulation of activated lymphocytes within lymph nodes, thymus, and the splenic white pulp, which obscured the cortico-medullary com-

P. Waterhouse, J. M. Penninger, E. Timms, A. Wakeham, A. Shahinian, T. W. Mak, Amgen Institute, Ontario Cancer Institute, Departments of Immunology and Medical Biophysics, University of Toronto, Toronto, Ontario M5G 2C1, Canada.
K. P. Lee and C. B. Thompson, Howard Hughes Medical Institute, Gwen Knapp Center, University of Chicago, Chicago, IL, 60637, USA.
H. Griesser, Department of Pathology, University of Toronto, Toronto, Ontario M5G 2C1, Canada.
*To whom correspondence should be addressed.